

Interoperability in encoded quantum repeater networks

Shota Nagayama,^{1,*} Byung-Soo Choi,² Simon Devitt,³ Shigeya Suzuki,⁴ and Rodney Van Meter⁵

¹*Graduate School of Media and Governance, Keio University,
5322 Endo, Fujisawa-shi, Kanagawa 252-0882, Japan*

²*Research Center for Quantum Information Technology,*

Electronics and Telecommunications Research Institute, Daejeon, South Korea

³*Center for Emergent Matter Science, RIKEN, Wako, Saitama 351-0198, Japan*

⁴*Keio Research Institute at SFC, Keio University,*

5322 Endo, Fujisawa-shi, Kanagawa 252-0882, Japan

⁵*Faculty of Environment and Information Studies, Keio University,*

5322 Endo, Fujisawa-shi, Kanagawa 252-0882, Japan

(Dated: September 16, 2018)

The future of quantum repeater networking will require interoperability between various error correcting codes. A few specific code conversions and even a generalized method are known, however, no detailed analysis of these techniques in the context of quantum networking has been performed. In this paper, we analyze a generalized procedure to create Bell pairs encoded heterogeneously between two separate codes used often in error corrected quantum repeater network designs. We begin with a physical Bell pair, then encode each qubit in a different error correcting code, using entanglement purification to increase the fidelity. We investigate three separate protocols for preparing the purified encoded Bell pair. We calculate the error probability of those schemes between the Steane $[[7,1,3]]$ code, a distance three surface code and single physical qubits by Monte Carlo simulation under a standard Pauli error model, and estimate the resource efficiency of the procedures. A local gate error rate of 10^{-3} allows us to create high-fidelity logical Bell pairs between any of our chosen codes. We find that a postselected model, where any detected parity flips in code stabilizers result in a restart of the protocol, performs the best.

I. INTRODUCTION

Much like the Internet of today, it is probable that a future Quantum Internet will be a collection of radically different quantum networks utilizing some form of quantum inter-networking. These networks, called *Autonomous Systems* in the classical Internet vernacular, are deployed and administered independently, and realize end-to-end communication by relaying their communication in a technology-independent, distributed fashion for scalability. In the quantum regime, different error mitigation techniques may be employed within neighboring quantum networks and a type of code conversion or code teleportation between heterogeneous error correcting codes must be provided for interoperability.

The quantum repeater is a core infrastructure component of a quantum network, tasked with constructing distributed quantum states or relaying quantum information as it routes from the source to the destination [1–4]. The quantum repeater creates new capabilities: end-to-end quantum communication, avoiding limitations on distance and the requirement for trust in quantum key distribution networks [5–7], wide-area cryptographic functions [8], distributed computation [9–15] and possibly use as physical reference frames [16–19].

Several different classes of quantum repeaters have been proposed [20–22] and these class distinctions often relate to how classical information is exchanged when

either preparing a connection over multiple repeaters, or sending a piece of quantum information from source to destination. The first class utilizes purification and swapping of physical Bell pairs [23–26]. First, neighboring repeaters establish raw (low fidelity) Bell pairs which are recursively used to purify a single pair to a desired fidelity. Adjacent stations then use entanglement swapping protocols to double the total range of the entanglement. In purify/swap protocols, classical information is exchanged continuously across the entire network path to herald failures of both purification protocols and entanglement swapping. This exchange of information limits the speed of such a network significantly, especially over long distances. The second class utilizes quantum error correction throughout the end-to-end communication [27–30] and limits the exchange of classical information to either two-way communications between adjacent repeaters or to ballistic communication, where the classical information flow is unidirectional from source to receiver. These approaches depend on either high probability of success for transmitting photons over a link with high fidelity, or build on top of heralded creation of nearest neighbor Bell pairs and purification, if necessary. If the probability of successful connection between adjacent repeaters is high enough we can use quantum error correcting codes and relax constraints on the technology, especially memory decoherence times and the need for large numbers of qubits in individual repeaters, by sending logically encoded states hop by hop in a quasi-asynchronous fashion [27, 31] or using speculative or measurement-based operations [30–32].

Independent networks may employ any of the above

* kurosagi@sfc.wide.ad.jp

schemes, and within some schemes may choose different error correcting codes or code distances. Initially deployed to support different applications and meet technological, logistical, geographic and economic constraints, they may use different physical implementations and will have different optimal choices for operational methods.

Over time, however, it will likely become desirable to interconnect these networks into a single, larger, internet-work. In this paper, we address the problem of creating end-to-end entanglement despite differences at the logical level.

These inter-network and differing operating environments can be bridged through the use of heterogeneously encoded logical Bell pairs, using separate error correction methods on each half of the pair. The idea of code conversion goes back a decade for use in large-scale systems. To achieve interoperability between two QEC codes, we can classify approaches into two groups, direct code conversion and code teleportation. Direct code conversion transforms an encoded state $|\psi\rangle_L$ into an encoded state $|\psi\rangle_{L'}$ where L and L' indicate two distinct codes. Since this change operates on valuable data, the key point is to find an appropriate fault-tolerant sequence that will convert the stabilizers from one code to the other [33–35]. In code teleportation, conversion is achieved by teleporting information using a heterogeneously encoded Bell pair as a resource state. Therefore, the key point is the method for preparing such a state.

Figure 1 shows an example use case for heterogeneously encoded Bell pairs, used in quantum *autonomous systems* [36]. Quantum *autonomous systems* of different codes interoperate via quantum repeaters building heterogeneously encoded Bell pairs.

In this paper, we give the first detailed analysis of the generalized approach to create heterogeneously encoded Bell pairs for interoperability of quantum error correcting networks. We evaluate this approach between the Steane $[[7,1,3]]$ code, a distance three surface code, and unencoded (raw) physical qubits. Figure 2 depicts a quantum repeater building and using heterogeneously encoded Bell pairs to be used in a quantum repeater.

We have studied three possible schemes to increase the fidelity of the heterogeneously encoded Bell pairs: *purification before encoding*, *purification after encoding* and *purification after encoding with strict post-selection*. *Purification before encoding* does entanglement purification at the level of physical Bell pairs. *Purification after encoding* does entanglement purification at the level of encoded Bell pairs. *Purification after encoding with strict post-selection* also does entanglement purification at the level of encoded Bell pairs. The difference from the previous scheme is that encoded Bell pairs in which any eigenvalue (error syndrome) of -1 is measured in the purification stage are discarded and the protocols restarted. We determine the error probability and the resource efficiency of these schemes by Monte Carlo simulation with the Pauli error model of circuit level noise [37].

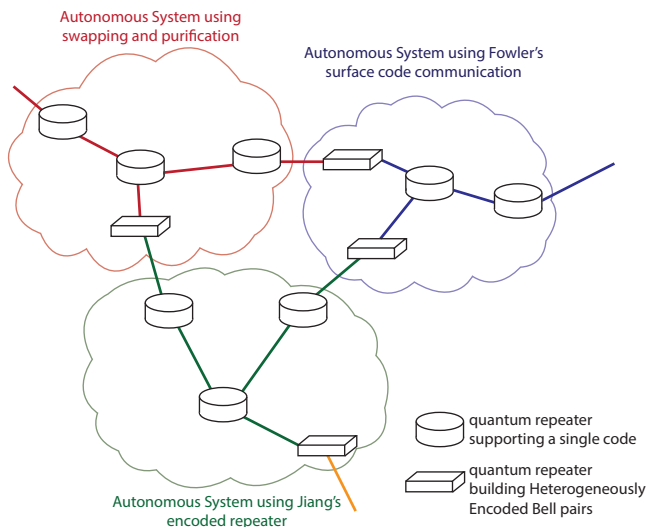


FIG. 1. A use case for quantum repeaters building heterogeneously encoded Bell pairs. Each cloud represents a quantum *autonomous system* which is based on an error correcting code or entanglement swapping and purification. Colored links are connections using those codes. Boxes are quantum repeaters building heterogeneously encoded Bell pairs. Cylinders are quantum repeaters, each of which supports only a single code. All links from a homogeneous repeater (cylinder) are the same type (color) since only quantum repeaters building heterogeneously encoded Bell pairs (boxes) can interoperate between different codes.

II. HETEROGENEOUSLY ENCODED BELL PAIRS

There are two methods for building heterogeneously encoded Bell pairs for code teleportation. The first is to inject each qubit of a physical Bell pair to a different code [38]. The second is to prepare a common cat state for two codes to check the ZZ parity of two logical qubits [39–41]. It has been shown that code teleportation utilizing a cat state is better than direct code conversion because the necessary stabilizer checking for the latter approach is too expensive [42]. Direct code conversion and code teleportation utilizing a cat state are specific for a chosen code pair as the specific sequence of fault-tolerant operations has to match the two codes chosen. In contrast, code teleportation by injecting a physical Bell pair can be used for any two codes, and provided encoding circuits are available for the two codes in question, the protocol can be generalized to arbitrary codes.

Putting things together, heterogeneous Bell pairs of long distance can be created by entanglement swapping (physical or logical) or a method appropriate to each network, allowing an arbitrary quantum state encoded in some code to be moved onto another code by teleportation [28, 29]. In a single computer, code conversion has been proposed for memory hierarchies and for cost-effective fault tolerant quantum computation

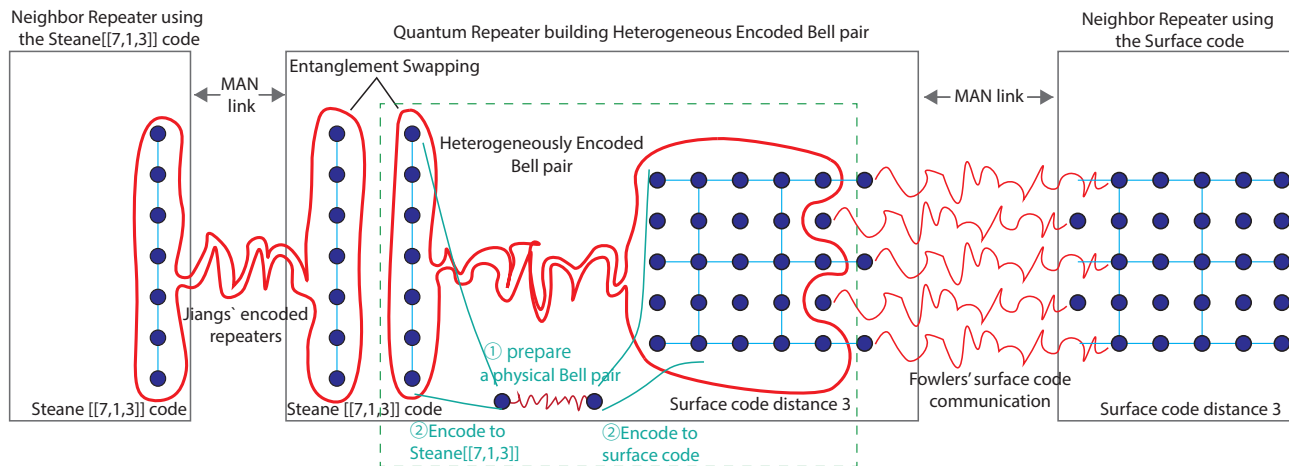


FIG. 2. Heterogeneously encoded Bell pairs can be used to bridge quantum networks using different error correcting mechanisms. MAN stands for metropolitan area network. A blue dot denotes a physical qubit. A set of blue lines indicates qubits which comprise an encoded qubit. Each thin red line describes an entanglement between encoded qubits. The half of the Bell pair encoded in the surface code can be sent to the neighboring quantum repeater by Fowler *et al.*'s method [29]. The other half of the Bell pair, encoded in the Steane $[[7,1,3]]$ code, undergoes entanglement swapping with a Steane $[[7,1,3]]$ -Steane $[[7,1,3]]$ encoded Bell pair established via Jiang *et al.*'s method [28]. Therefore this central quantum repeater can create entanglement between the two quantum repeaters in different types of networks. In the green dashed rectangle is the procedure for encoding a Bell pair heterogeneously. A qubit of a Bell pair is encoded onto Steane $[[7,1,3]]$ on the left side of the figure, adding 6 qubits. The other qubit of the Bell pair is encoded onto the surface code of distance 3, adding 24 qubits on the right side of the figure. Multiple copies are prepared, entangled and purified. Eventually, a heterogeneously encoded logical Bell pair is achieved with high enough fidelity to enable coupling of the two networks.

[33, 38, 40, 43–45].

The green dashed rectangle in Figure 2 shows the basic procedure for creating a heterogeneously encoded logical Bell pair. Each dot denotes a physical qubit and thin blue lines connecting those dots demarcate the set of physical qubits comprising a logical qubit. Each qubit of a Bell pair is processed separately and encoded onto its respective code through non-fault-tolerant methods to create arbitrary encoded states. Figure 3 shows the circuit to encode an arbitrary quantum state in the Steane $[[7,1,3]]$ code [46, 47]. Figure 4 shows the circuit to encode an arbitrary quantum state in the surface code [49]. The KQ of a circuit is the number of qubits times the circuit depth, giving an estimate of the number of opportunities for errors to occur [46]. Note that those circuits are not required to be fault-tolerant because the state being purified is generic, rather than irreplaceable data. If the fidelity of the encoded Bell pair is not good enough (e.g. as determined operationally using quantum state tomography), entanglement purification is performed [50, 51].

III. THREE METHODS TO PREPARE A HETEROGENEOUSLY ENCODED HIGH FIDELITY BELL PAIR

Entanglement purification is performed to establish high fidelity entanglement [52, 53]. Entanglement purification can be viewed as a distributed procedure for

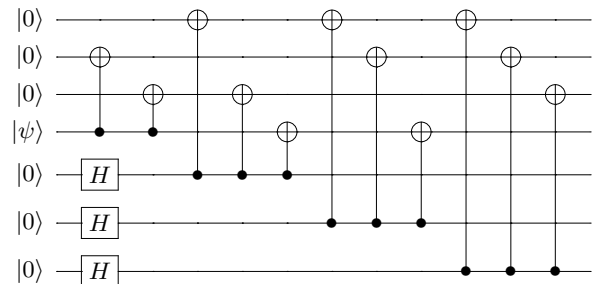


FIG. 3. Circuit to encode an arbitrary state to the Steane $[[7,1,3]]$ code [48]. $|\psi\rangle$ is the state to be encoded. This circuit is not fault-tolerant. The KQ of this circuit is 42 because some gates can be performed simultaneously.

testing a proposition about a distributed state [21].

Figure 5 shows the circuit for the basic form of entanglement purification where $|\phi\rangle$ is a noisy Bell pair. The input is two low fidelity Bell pairs and on success the output is a Bell pair of higher fidelity. One round of purification suppresses one type of error, X or Z. If the initial Bell pairs are Werner states, or approximately Werner states, then to suppress both types, two rounds of purification are required. The first round makes the resulting state into a binary state with only one signifi-

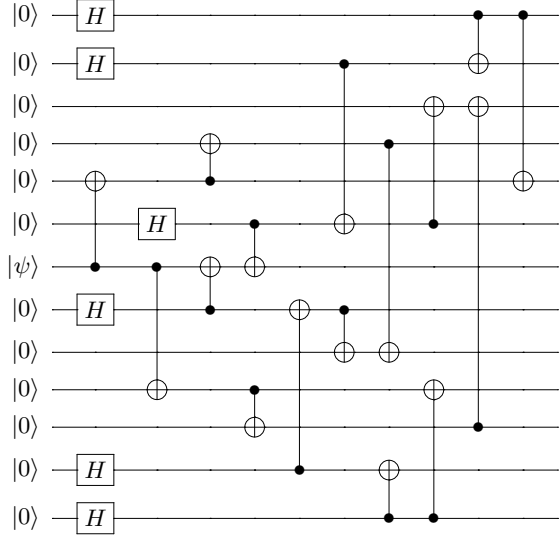


FIG. 4. Circuit to encode an arbitrary state $|\psi\rangle$ to a distance three surface code [49]. This circuit is not fault-tolerant. The KQ of this circuit is 250 if some gates are performed simultaneously.

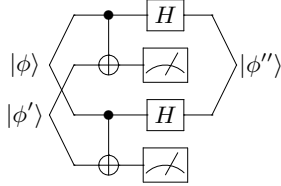


FIG. 5. Circuit for entanglement purification [2]. The two measured values are compared. If they disagree, the output qubits are discarded. If they agree, the output qubits are treated as a new Bell pair. At this point, the X error rate of the output Bell pair is suppressed from the input Bell pairs. The Hadamard gates exchange the X and Z axes, so that the following round of purification suppresses the Z error rate. As the result, entanglement purification consumes two Bell pairs and generates a Bell pair of higher fidelity stochastically.

cant error term but not a significantly improved fidelity. The second round then strongly suppresses errors if the gate error rate is small. Thus, the overall fidelity tends to improve in a stair step fashion. After two rounds of purification, the distilled fidelity will be, in the absence of local gate error,

$$F'' \sim \frac{F^2}{F^2 + (1 - F)^2} \quad (1)$$

where the original state is the Werner state

$$\rho = F|\Phi^+\rangle\langle\Phi^+| + \frac{1-F}{3}(|\Phi^-\rangle\langle\Phi^-| + |\Psi^+\rangle\langle\Psi^+| + |\Psi^-\rangle\langle\Psi^-|) \quad (2)$$

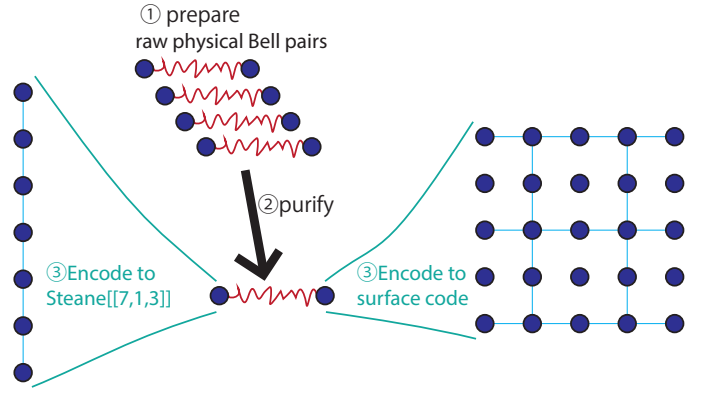


FIG. 6. Overview of the scheme which purifies physical Bell pairs to generate an encoded Bell pair of high fidelity. First, entanglement purification is conducted between physical Bell pairs an arbitrary number of times. Second, each qubit of the purified physical Bell pair is encoded to heterogeneous error correcting code.

and F is the fidelity $F = \langle\phi|\rho|\phi\rangle$ if $|\phi\rangle$ is the desired state. The probability of success of a round of purification is

$$p = F^2 + 2F\frac{1-F}{3} + 5\left(\frac{1-F}{3}\right)^2. \quad (3)$$

Table I in the appendix provides the numerical data for this to compare with our protocols. Our simulation assumptions are detailed in section IV.

A. Purification before encoding

Figure 6 shows the overview of the scheme to make heterogeneously encoded Bell pairs that are purified before encoding. To create an encoded Bell pair of high fidelity, entanglement purification is repeated the desired number of times. Next, each qubit of the purified Bell pair is encoded to its respective error correcting code. To estimate the rate of *logical* error after encoding, we perform a perfect syndrome extraction of the system to remove any residual correctable errors. After the whole procedure finishes, we check whether logical errors exist. Table II in the appendix presents the details of the simulated error probability and resource efficiency of *purification before encoding*.

B. Purification after encoding

Figure 7 shows the overview of the scheme to make heterogeneously encoded Bell pairs that are purified after encoding. In this scheme, to create an encoded Bell pair of high fidelity, heterogeneously encoded Bell pairs are generated first by encoding each qubit of a raw physical Bell pair to our chosen heterogeneous error correcting

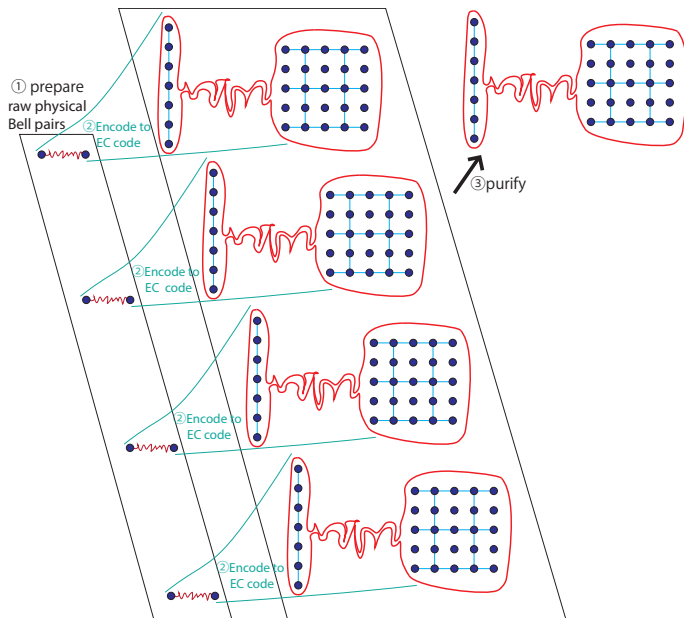


FIG. 7. Overview of the scheme which purifies encoded Bell pairs to achieve an encoded Bell pair of high fidelity. In this method, first, raw physical Bell pairs are encoded into our heterogeneous error correcting code, Secondly, those heterogeneously encoded Bell pairs are purified directly at the logical level.

codes. Next, those encoded Bell pairs are purified at the logical level the desired number of times, via transversal CNOTs and logical measurements. Table III presents the details of the simulated error probability and resource efficiency of *purification after encoding*.

C. Purification after encoding with strict post-selection

Figure 8 shows the overview of the scheme to make encoded Bell pairs, purified after encoding with strict post-selection protocols to detect errors. This scheme uses a procedure similar to *purification after encoding*. In this scheme, to create an encoded Bell pair of high fidelity, heterogeneously encoded Bell pairs are generated first by encoding each qubit of a raw physical Bell pair to our chosen heterogeneous error correcting codes. We then run purification protocols at the logical level, similarly to the previous protocol. However, when we perform a logical measurement as part of this protocol, we also calculate (classically) the eigenvalues of all code stabilizers. If any

of these eigenvalues are found to be negative, we treat the operation as a failure (in a similar manner to odd parity logical measurements for the purification) and the output Bell pair of the purification is discarded. This simultaneously performs purification and error correction using the properties of the codes. Table IV presents the details of the numerically calculated error probability and resource efficiency of *purification after encoding with strict*

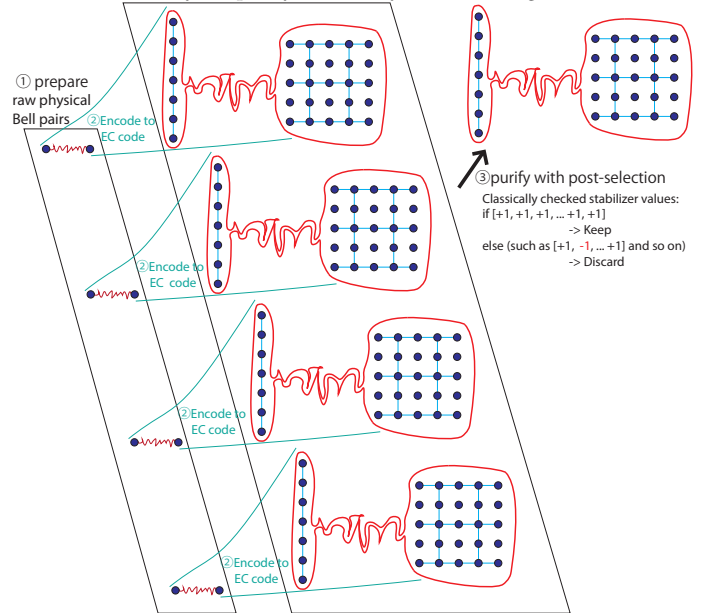


FIG. 8. Overview of the scheme which purifies encoded Bell pairs to achieve an encoded Bell pair of high fidelity with strict post-selection. First, raw physical Bell pairs are encoded to heterogeneous error correcting code, same as *purification after encoding*. Secondly, at measurement in purification, eigenvalues of each stabilizer are checked classically. If any eigenvalue of -1 is measured, the output Bell pair is discarded (in a similar manner to if the overlying purification protocol failed).

post-selection.

IV. ERROR SIMULATION AND RESOURCE ANALYSIS

We calculate the error probability and estimate resource requirements by Monte Carlo simulation. The physical Bell pairs' fidelity is assumed to be 0.85; the state is assumed to be, following Nölleke *et al.* [54],

$$\rho = 0.85|\Phi^+\rangle\langle\Phi^+| + 0.04|\Phi^-\rangle\langle\Phi^-| + 0.055|\Psi^+\rangle\langle\Psi^+| + 0.055|\Psi^-\rangle\langle\Psi^-|. \quad (4)$$

Our error model is the Pauli model of circuit level noise [37]. This model consists of memory error, 1-qubit

gate error, 2-qubit gate error, and measurement error

each of which occurs with the error probability p . Memory, 1-qubit gates and measurement are all vulnerable to X, Y and Z errors and we assume a balanced model, where probabilities are $\frac{p}{3}$ respectively. Similarly, 2-qubit gates are vulnerable to all fifteen possibilities, each with a probability of $\frac{p}{15}$. Errors propagate during all circuits after the initial distribution of Bell pairs.

Figure 9 plots the numbers of consumed raw physical Bell pairs versus logical error rate in the output state.

The numbers of raw Bell pairs consumed declines as the local gate error rate is lowered. This is because the influence of the local gate error rate shrinks relative to the infidelity of generated raw Bell pairs. If the system is free from local gate error, the numbers of raw Bell pairs consumed by the three schemes must converge. At $p = 10^{-5}$, the required number of raw Bell pairs of the schemes are essentially identical and they require about 26 raw Bell pairs to achieve four rounds of purification. Higher efficiency would require improving the initial fidelity of $F = 0.85$.

At any error rate and with any number of rounds of purification from 0 to 4, *purification before encoding* and *purification after encoding* result in fidelity worse than simple purification of physical Bell pairs. This suggests that errors accumulated during encoding are difficult to correct. On the other hand, *purification after encoding with strict post-selection* gives better results than simple purification, at the expense of consuming more raw physical Bell pairs. This difference is noticeable at $p = 10^{-3}$; 51 raw physical Bell pairs are used to create an encoded Bell pair purified four rounds. The local gate error rate is so high that an eigenvalue of -1 is often found at the measurement in purification and the output Bell pair is discarded. For *purification after encoding with post-selection*, the residual error rate after n rounds of purification is similar at any p , but resource demands change. It converts local errors into “loss”, or discarded states. Therefore *purification after encoding with post-selection* is dominated by the original raw Bell pair infidelity. At $p = 10^{-3}$, *purification after encoding* also requires more raw physical Bell pairs than the other schemes, because the error rate after purification is so high that the success probability of purification is poor.

Though more rounds of purification are supposed to result in smaller logical error rate, three rounds of purification of *purification after encoding* at $p = 10^{-3}$ give an error rate *larger* than that of two rounds. The local gate error rate is too high and purification introduces more errors than it suppresses on odd-numbered purification rounds.

Purification after encoding with strict post-selection gives similar results for the two local gate error rates $p = 10^{-4}$ and $p = 10^{-5}$. The difference is a small number of consumed raw physical Bell pairs. From this fact we conclude that $p = 10^{-3}$ is a good enough local gate error rate to allow us to create heterogeneously encoded Bell pairs from raw physical Bell pairs of $F=0.85$.

V. DISCUSSION

We have proposed and analysed a generalized method for creating heterogeneously encoded Bell pairs that can be used for interoperability between encoded networks. This is the first step in examining the full design of interconnection routers for quantum repeater systems utilizing different error mitigation techniques. Our results have shown that *purification after encoding with strict post-selection* is a better preparation method than our other two candidates. Strict post-selection of two rounds of purification results in better fidelity than error correction of four rounds of purification at all error rates, and better physical Bell pair efficiency. Since the threshold of the error rate of the Steane [[7,1,3]] code is around 10^{-4} , our simulations of *purification before encoding* and *purification after encoding* of $\sim 10^{-4}$ do not show an advantage compared to simple physical purification; however, strict post-selection does. *Purification after encoding with strict post-selection* has a higher threshold than the normal encoding and purification do. With initial $F = 0.85$, we can reach error rate of 10^{-3} (good enough for distributed numeric computation) using 4 rounds of purification, for physical Bell pairs at $p = 10^{-5}$ or post-selected heterogeneous pairs at $p = 10^{-4}$.

As we noted in the introduction, quantum repeater networks will serve several purposes, potentially requiring different residual error levels on the end-to-end quantum communication. Networks using physical purify-and-swap technologies, for example, will easily support QKD, but distributed numeric computation will require building error correction on top of the Bell pairs provided by the network. Our simulations of heterogeneous Bell pairs where one half is a physical qubit, rather than logically encoded, are described in the appendix. These simulations show that residual error rates can be suppressed successfully, allowing us to bridge these separate types of networks and support the deployment of any application suitable for purify-and-swap networks across a heterogeneous quantum Internet. The error rates we have achieved for each heterogeneous technology pair demonstrate the effectiveness of our heterogeneous scheme for interoperability. Moreover, operation appears to be feasible at a local gate error rate of 10^{-3} , and at 10^{-4} operation is almost indistinguishable from having perfect local gates.

The analysis presented here is useful not only in the abstract, but also serves as a first step toward a hardware design for a multi-protocol quantum router (the boxes in Figure 1). Such a router may be built on a quantum multicomputer architecture, with several small quantum computers coupled internally via a local optical network [55–58]. This allows hardware architects to build separate, small devices to connect to each type of network, then to create Bell pairs between these devices using the method described in this paper. In addition, this method can be used within large-scale quantum computers that wish to use different quantum error correcting

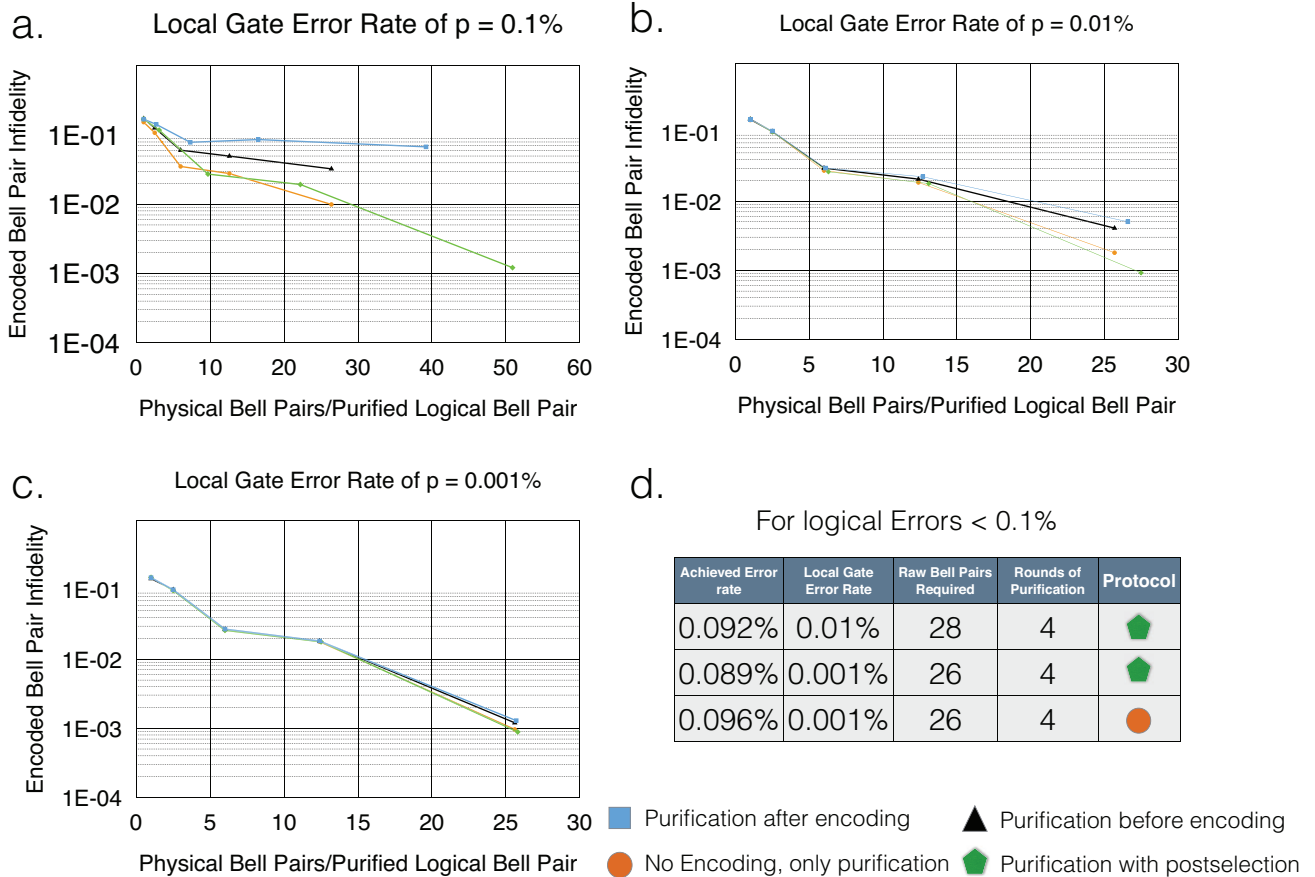


FIG. 9. Results of simulation of creation of a Steane $[[7,1,3]]$ -surface code distance 3 heterogeneous Bell pair, showing residual logical error rate versus physical Bell pairs consumed. The three schemes plus the baseline case of purification of physical Bell pairs are each represented by a line. Each point along a line corresponds to the number of rounds of purification. The leftmost point represents no purification, the second point is one round of purification, and the rightmost point represents four rounds of purification a.-c. Improving values of local gate error rate. d. The three cases with residual error rate of 10^{-3} or less.

codes for different purposes, such as long-term memory or ancilla state preparation.

This scheme is internal to a single repeater at the border of two networks, and will allow effective end-to-end communication where errors across links are more important than errors within a repeater node. It therefore can

serve as a building block for a quantum Internet.

ACKNOWLEDGEMENT

This work is supported by JSPS KAKENHI Grant Number 25280034 and 25:4103. We thank Joe Touch for valuable technical conversations.

[1] H.-J. Briegel, W. Dür, J. Cirac, and P. Zoller, *Phys. Rev. Lett.* **81**, 5932 (1998).
 [2] W. Dür, H.-J. Briegel, J. I. Cirac, and P. Zoller, *Physical Review A* **59**, 169 (1999).
 [3] R. Van Meter, *Network*, IEEE **26**, 59 (2012).
 [4] H. J. Kimble, *Nature* **453**, 1023 (2008).
 [5] C. Elliott, A. Colvin, D. Pearson, O. Pikalo, J. Schlafer, and H. Yeh, “Current status of the DARPA quantum network (invited paper),” (*Proc. SPIE* 5815, 2005).

[6] M. Peev, C. Pacher, R. Allaupe, C. Barreiro, J. Bouda, W. Boxleitner, T. Debuisschert, E. Diamanti, M. Dianati, J. F. Dynes, S. Fasel, S. Fossier, M. Frst, J.-D. Gautier, O. Gay, N. Gisin, P. Grangier, A. Happe, Y. Hasani, M. Hentschel, H. Hübel, G. Humer, T. Länger, M. Legr, R. Lieger, J. Lodewyck, T. Lornser, N. Ltkenhaus, A. Marhold, T. Matyus, O. Maurhart, L. Monat, S. Nauerth, J.-B. Page, A. Poppe, E. Querasser, G. Ribordy, S. Robyr, L. Salvail, A. W. Sharpe, A. J. Shields,

- D. Stucki, M. Suda, C. Tamas, T. Themel, R. T. Thew, Y. Thoma, A. Treiber, P. Trinkler, R. Tualle-Brouiri, F. Vannel, N. Walenta, H. Weier, H. Weinfurter, I. Wimberger, Z. L. Yuan, H. Zbinden, and A. Zeilinger, *New Journal of Physics* **11**, 075001 (2009).
- [7] M. Sasaki, M. Fujiwara, H. Ishizuka, W. Klaus, K. Wakui, M. Takeoka, S. Miki, T. Yamashita, Z. Wang, A. Tanaka, K. Yoshino, Y. Nambu, S. Takahashi, A. Tajima, A. Tomita, T. Domeki, T. Hasegawa, Y. Sakai, H. Kobayashi, T. Asai, K. Shimizu, T. Tokura, T. Tsurumaru, M. Matsui, T. Honjo, K. Tamaki, H. Takesue, Y. Tokura, J. F. Dynes, A. R. Dixon, A. W. Sharpe, Z. L. Yuan, A. J. Shields, S. Uchikoga, M. Legré, S. Robyr, P. Trinkler, L. Monat, J.-B. Page, G. Ribordy, A. Poppe, A. Allacher, O. Maurhart, T. Länger, M. Peev, and A. Zeilinger, *Opt. Express* **19**, 10387 (2011).
- [8] M. Ben-Or and A. Hassidim, in *Proceedings of the Thirty-seventh Annual ACM Symposium on Theory of Computing*, STOC '05 (ACM, New York, NY, USA, 2005) pp. 481–485.
- [9] H. Buhrman, R. Cleve, S. Massar, and R. de Wolf, *Rev. Mod. Phys.* **82**, 665 (2010).
- [10] H. Buhrman and H. Röhrig, “Mathematical foundations of computer science 2003,” (Springer-Verlag, 2003) Chap. Distributed Quantum Computing, pp. 1–20.
- [11] H. Buhrman, R. Cleve, and A. Wigderson, in *Proceedings of the thirtieth annual ACM symposium on Theory of computing* (ACM, 1998) pp. 63–68.
- [12] C. Monroe, R. Raussendorf, A. Ruthven, K. R. Brown, P. Maunz, L.-M. Duan, and J. Kim, *Phys. Rev. A* **89**, 022317 (2014).
- [13] C.-H. Chien, R. Van Meter, and S.-Y. Kuo, “Fault-tolerant operations for universal blind quantum computation,” (2015), to appear; preprint available as arXiv:1306.3664 [quant-ph].
- [14] A. Broadbent, J. Fitzsimons, and E. Kashefi, in *Formal Methods for Quantitative Aspects of Programming Languages* (Springer, 2010) pp. 43–86.
- [15] C. Crépeau, D. Gottesman, and A. Smith, in *STOC 2002*.
- [16] R. Jozsa, D. Abrams, J. Dowling, and C. Williams, *Physical Review Letters* **85**, 2010 (2000).
- [17] P. Kómar, E. Kessler, M. Bishof, L. Jiang, A. S. Sorensen, and M. D. Lukin, *Nature Physics* (2014), 10.1038/NPHYS3000.
- [18] I. Chuang, *Physical Review Letters* **85**, 2006 (2000).
- [19] S. D. Bartlett, T. Rudolph, and R. W. Spekkens, *Rev. Mod. Phys.* **79**, 555 (2007).
- [20] W. J. Munro, S. J. Devitt, and K. Nemoto, in *SPIE Optical Engineering+ Applications* (International Society for Optics and Photonics, 2011) pp. 816307–816307.
- [21] R. Van Meter, *Quantum Networking* (WILEY, 2014).
- [22] M. Takeoka, S. Guha, and M. M. Wilde, *Nature communications* **5** (2014).
- [23] L.-M. Duan, M. D. Lukin, J. I. Cirac, and P. Zoller, *Nature* **414**, 413 (2001).
- [24] P. van Loock, T. D. Ladd, K. Sanaka, F. Yamaguchi, K. Nemoto, W. J. Munro, and Y. Yamamoto, *Phys. Rev. Lett.* **96**, 240501 (2006).
- [25] N. Sangouard, C. Simon, H. de Riedmatten, and N. Gisin, *Rev. Mod. Phys.* **83**, 33 (2011).
- [26] L. Jiang, J. M. Taylor, N. Khaneja, and M. D. Lukin, *Proceedings of the National Academy of Sciences* **104**, 17291 (2007), <http://www.pnas.org/content/104/44/17291.full.pdf>.
- [27] W. Munro, K. Harrison, A. Stephens, S. Devitt, and K. Nemoto, *Nature Photonics* **4**, 792 (2010).
- [28] L. Jiang, J. M. Taylor, K. Nemoto, W. J. Munro, R. Van Meter, and M. D. Lukin, *Phys. Rev. A* **79**, 032325 (2009).
- [29] A. G. Fowler, D. S. Wang, C. D. Hill, T. D. Ladd, R. Van Meter, and L. C. L. Hollenberg, *Phys. Rev. Lett.* **104**, 180503 (2010).
- [30] Y. Li, S. D. Barrett, T. M. Stace, and S. C. Benjamin, *New Journal of Physics* **15**, 023012 (2013).
- [31] W. J. Munro, A. M. Stephens, S. J. Devitt, K. A. Harrison, and K. Nemoto, *Nature Photonics* **6**, 777 (2012).
- [32] M. Zwerger, W. Dür, and H. J. Briegel, *Phys. Rev. A* **85**, 062326 (2012).
- [33] J. T. Anderson, G. Duclos-Cianci, and D. Poulin, *Phys. Rev. Lett.* **113**, 080501 (2014).
- [34] C. D. Hill, A. G. Fowler, D. S. Wang, and L. C. L. Hollenberg, *Quantum Info. Comput.* **13**, 439 (2013).
- [35] A. M. Stephens, Z. W. E. Evans, S. J. Devitt, and L. C. L. Hollenberg, *Phys. Rev. A* **77**, 062335 (2008).
- [36] In the classical Internet, significant differences may occur even between subnets of a single AS, but for simplicity in this paper we will restrict ourselves to the assumption that a quantum AS is internally homogeneous.
- [37] A. J. Landahl, J. T. Anderson, and P. R. Rice, arXiv preprint arXiv:1108.5738 (2011).
- [38] D. Copley, M. Oskin, F. T. Chong, I. Chuang, and K. Abdel-Gaffar, in *1st Workshop on Non-Silicon Computing* (2002).
- [39] M. Oskin, F. Chong, and I. Chuang, *Computer* **35**, 79 (2002).
- [40] D. D. Thaker, T. S. Metodi, A. W. Cross, I. L. Chuang, and F. T. Chong, *SIGARCH Comput. Archit. News* **34**, 378 (2006).
- [41] T. S. Metodi, A. I. Faruque, and F. T. Chong, *Synthesis Lectures on Computer Architecture* **6**, 1 (2011).
- [42] B.-S. Choi, in *ICT Convergence (ICTC), 2013 International Conference on* (2013) pp. 1083–1087.
- [43] T. Joehym-O’Connor and R. Laflamme, *Phys. Rev. Lett.* **112**, 010505 (2014).
- [44] A. Paetznick and B. W. Reichardt, *Phys. Rev. Lett.* **111**, 090505 (2013).
- [45] B.-S. Choi, *Quantum Information Processing* **1570-0755**, 2775 (2015).
- [46] A. Steane, *Proceedings of the Royal Society of London A: Mathematical, Physical and Engineering Sciences* **452**, 2551 (1996).
- [47] A. M. Steane, *Nature* **399**, 124 (1999).
- [48] S. Buchbinder, C. Huang, and Y. Weinstein, *Quantum Information Processing* **12**, 699 (2013).
- [49] E. Dennis, A. Kitaev, A. Landahl, and J. Preskill, *Journal of Mathematical Physics* **43** (2002).
- [50] S. Bravyi and A. Kitaev, *Physical Review A* **71**, 22316 (2005).
- [51] M. Kleinmann, H. Kampermann, T. Meyer, and D. Bruß, *Phys. Rev. A* **73**, 062309 (2006).
- [52] W. Dür and H.-J. Briegel, *Phys. Rev. Lett.* **90**, 067901 (2003).
- [53] W. Dür and H. Briegel, *Rep. Prog. Phys.* **70**, 1381 (2007).
- [54] C. Nölleke, A. Neuzner, A. Reiserer, C. Hahn, G. Rempe, and S. Ritter, *Phys. Rev. Lett.* **110**, 140403 (2013).

- [55] R. Van Meter, T. D. Ladd, A. G. Fowler, and Y. Yamamoto, *International Journal of Quantum Information* **8**, 295 (2010).
- [56] L. Jiang, J. M. Taylor, A. S. Sørensen, and M. D. Lukin, *Phys. Rev. A* **76**, 062323 (2007).
- [57] J. Kim and C. Kim, *Quantum Information and Computation* **9** (2009).
- [58] D. K. L. Oi, S. J. Devitt, and L. C. L. Hollenberg, *Physical Review A* **74**, 052313 (2006).

Appendix A: Detailed Data

Table I shows our baseline simulation results using physical entanglement only with no encoding. Table II shows the simulated results of *purification before encoding* for a Bell pair of a single layer of the Steane $[[7,1,3]]$ code and a distance 3 surface code. Table III shows the

simulated results of the scheme *purification after encoding* of the same codes. Table IV shows the simulated results of the scheme *purification after encoding with strict post-selection*. Since purification at the level of encoded qubits consists of logical gates, *purification before encoding* has a much smaller KQ than the other two schemes. *Purification after encoding with strict post-selection* discards more qubits than *purification after encoding* does to create a purified encoded Bell pair, so that *purification after encoding with strict post-selection* also results in a larger KQ. Table V shows the simulated results of the scheme *purification after encoding with strict post-selection* between the Steane $[[7,1,3]]$ code and the non-encoded physical half. Table VI shows the simulated results of the scheme *purification after encoding with strict post-selection* between the distance three surface code and the non-encoded physical half.

TABLE I. Our baseline case, discrete simulation using physical entanglement purification only. The merged error rate is the probability that either X error or Z error occurs. The physical Bell pair inefficiency is $(\# \text{ created raw Bell pairs})/(\# \text{ purified Bell pairs})$. KQ is $\# \text{qubit} \times \# \text{steps}$. In this simulation, KQ is the number of chances that errors may occur.

(a)The local gate error rate is 10^{-3} .

#purification	X error rate	Z error rate	Merged error rate	Phys. Bell Pair Ineff.	KQ	#single qubit gate	#two qubit gate
0	0.112	0.0999	0.154	1.0	88	86	1
1	0.0979	0.0201	0.108	2.5	98	91	5
2	0.0248	0.0145	0.0352	6.0	122	103	14
3	0.0251	0.00501	0.0278	12.6	167	126	32
4	0.0073	0.00491	0.00993	26.4	262	173	70

(b)The local gate error rate is 10^{-4} .

#purification	X error rate	Z error rate	Merged error rate	Phys. Bell Pair Ineff.	KQ	#single qubit gate	#two qubit gate
0	0.11	0.096	0.15	1.0	88	86	1
1	0.0927	0.0159	0.101	2.5	98	91	5
2	0.0187	0.011	0.0278	6.0	121	103	14
3	0.0182	0.000791	0.0187	12.4	166	125	32
4	0.00126	0.000758	0.00179	25.7	258	171	68

(c)The local gate error rate is 10^{-5} .

#purification	X error rate	Z error rate	Merged error rate	Phys. Bell Pair Ineff.	KQ	#single qubit gate	#two qubit gate
0	0.109	0.0961	0.15	1.0	88	86	1
1	0.0926	0.0153	0.1	2.5	98	91	5
2	0.0178	0.0102	0.0264	6.0	121	103	14
3	0.0176	0.000369	0.0179	12.4	166	125	32
4	0.000635	0.000353	0.000963	25.6	257	171	68

TABLE II. Simulation results of *purification before encoding* for a Bell pair of a single layer of the Steane $[[7,1,3]]$ code and a distance 3 surface code. Other conditions and definitions are as in Table I.

(a)The local gate error rate is 10^{-3} .

#purification	X error rate	Z error rate	Merged error rate	Phys. Bell Pair Ineff.	KQ	#single qubit gate	#two qubit gate
0	0.121	0.108	0.173	1.0	5624	4328	648
1	0.106	0.0354	0.127	2.5	5634	4333	652
2	0.0365	0.0314	0.0605	6.0	5658	4345	661
3	0.0346	0.0206	0.0497	12.6	5703	4368	679
4	0.0181	0.0191	0.0325	26.4	5798	4415	717

(b)The local gate error rate is 10^{-4} .

#purification	X error rate	Z error rate	Merged error rate	Phys. Bell Pair Ineff.	KQ	#single qubit gate	#two qubit gate
0	0.112	0.0962	0.154	1.0	5624	4328	648
1	0.0927	0.0171	0.102	2.5	5634	4333	652
2	0.02	0.0123	0.0302	6.0	5658	4345	661
3	0.0192	0.00224	0.0209	12.4	5702	4367	679
4	0.00232	0.00222	0.00407	25.7	5794	4413	715

(c)The local gate error rate is 10^{-5} .

#purification	X error rate	Z error rate	Merged error rate	Phys. Bell Pair Ineff.	KQ	#single qubit gate	#two qubit gate
0	0.109	0.0913	0.146	1.0	5624	4328	648
1	0.0927	0.0156	0.101	2.5	5634	4333	652
2	0.0179	0.0106	0.0269	6.0	5657	4345	661
3	0.0177	0.000552	0.0182	12.4	5702	4367	679
4	0.000745	0.000497	0.0012	25.6	5793	4413	715

TABLE III. Simulation results of the scheme *purification after encoding* between the Steane $[[7,1,3]]$ code and the distance three surface code. Other conditions and definitions are as in Table I.

(a)The local gate error rate is 10^{-3} .

#purification	X error rate	Z error rate	Merged error rate	Phys. Bell Pair Ineff.	KQ	#single qubit gate	#two qubit gate
0	0.122	0.108	0.17	1.0	5624	4328	648
1	0.126	0.032	0.143	2.7	7516	6034	756
2	0.0448	0.0441	0.0787	7.3	12730	10735	1052
3	0.0744	0.0172	0.0862	16.5	23118	20099	1644
4	0.0341	0.0378	0.0676	39.2	48667	43129	3100

(b)The local gate error rate is 10^{-4} .

#purification	X error rate	Z error rate	Merged error rate	Phys. Bell Pair Ineff.	KQ	#single qubit gate	#two qubit gate
0	0.113	0.097	0.154	1.0	5624	4328	648
1	0.0958	0.0168	0.104	2.5	7334	5868	746
2	0.0194	0.0128	0.0302	6.1	11427	9554	981
3	0.0215	0.00147	0.0226	12.7	18984	16357	1416
4	0.00257	0.0027	0.00503	26.6	34861	30650	2329

(c)The local gate error rate is 10^{-5} .

#purification	X error rate	Z error rate	Merged error rate	Phys. Bell Pair Ineff.	KQ	#single qubit gate	#two qubit gate
0	0.111	0.0946	0.151	1.0	5624	4328	648
1	0.0938	0.0151	0.101	2.5	7311	5847	745
2	0.018	0.0108	0.0272	6.0	11294	9433	973
3	0.0179	0.000441	0.0183	12.4	18642	16047	1397
4	0.000769	0.000547	0.00129	25.7	33870	29755	2274

TABLE IV. Simulation results of the scheme *purification after encoding with strict post-selection* between the Steane $[[7,1,3]]$ code and the distance three surface code. Other conditions and definitions are as in Table I.

(a)The local gate error rate is 10^{-3} .

#purification	X error rate	Z error rate	Merged error rate	Phys. Bell Pair Ineff.	KQ	#single qubit gate	#two qubit gate
0	0.118	0.115	0.171	1.0	5624	4328	648
1	0.11	0.0159	0.118	3.1	7932	6410	778
2	0.0179	0.011	0.0273	9.7	15249	13011	1189
3	0.019	0.000398	0.0193	22.2	29090	25492	1969
4	0.000798	0.000423	0.00121	50.9	61048	54314	3769

(b)The local gate error rate is 10^{-4} .

#purification	X error rate	Z error rate	Merged error rate	Phys. Bell Pair Ineff.	KQ	#single qubit gate	#two qubit gate
0	0.112	0.0993	0.154	1.0	5624	4328	648
1	0.0935	0.0147	0.101	2.5	7366	5897	748
2	0.0179	0.0102	0.0267	6.3	11592	9702	990
3	0.0177	0.000327	0.018	13.1	19397	16730	1438
4	0.000575	0.000343	0.000915	27.5	35733	31437	2377

(c)The local gate error rate is 10^{-5} .

#purification	X error rate	Z error rate	Merged error rate	Phys. Bell Pair Ineff.	KQ	#single qubit gate	#two qubit gate
0	0.111	0.0983	0.152	1.0	5624	4328	648
1	0.0915	0.0144	0.0983	2.5	7318	5853	745
2	0.0176	0.00998	0.0261	6.0	11304	9442	974
3	0.0175	0.000321	0.0178	12.5	18687	16088	1399
4	0.000571	0.000317	0.000886	25.8	33957	29833	2279

TABLE V. Simulation results of the scheme *purification after encoding with strict post-selection* between the Steane $[[7,1,3]]$ code and non-encoded physical half. Other conditions and definitions are as in Table I.

(a)The local gate error rate is 10^{-3} .

#purification	X error rate	Z error rate	Merged error rate	Phys. Bell Pair Ineff.	KQ	#single qubit gate	#two qubit gate
0	0.112	0.106	0.161	1.0	4260	3660	300
1	0.103	0.0168	0.111	2.7	5370	4712	330
2	0.0213	0.0133	0.0324	6.9	8235	7426	409
3	0.0229	0.00141	0.0238	14.9	13687	12590	558
4	0.00283	0.00149	0.00382	32.4	25534	23813	883

(b)The local gate error rate is 10^{-4} .

#purification	X error rate	Z error rate	Merged error rate	Phys. Bell Pair Ineff.	KQ	#single qubit gate	#two qubit gate
0	0.109	0.0945	0.149	1.0	4260	3660	300
1	0.0926	0.0156	0.101	2.5	5283	4629	328
2	0.0182	0.0103	0.027	6.1	7706	6923	395
3	0.018	0.000419	0.0183	12.6	12204	11181	518
4	0.000792	0.000448	0.00119	26.2	21554	20033	775

(c)The local gate error rate is 10^{-5} .

#purification	X error rate	Z error rate	Merged error rate	Phys. Bell Pair Ineff.	KQ	#single qubit gate	#two qubit gate
0	0.109	0.0969	0.15	1.0	4260	3660	300
1	0.0927	0.015	0.0999	2.5	5275	4621	328
2	0.0181	0.0105	0.0271	6.0	7656	6875	393
3	0.0175	0.000334	0.0178	12.4	12069	11053	515
4	0.000572	0.000325	0.000895	25.7	21202	19700	766

TABLE VI. Simulation results of the scheme *purification after encoding with strict post-selection* between the distance three surface code and non-encoded physical half. Other conditions and definitions are as in Table I.

(a)The local gate error rate is 10^{-3} .

#purification	X error rate	Z error rate	Merged error rate	Phys. Bell Pair Ineff.	KQ	#single qubit gate	#two qubit gate
0	0.124	0.109	0.172	1.0	1296	998	149
1	0.111	0.018	0.12	2.9	2303	1859	237
2	0.023	0.0137	0.0342	8.2	5180	4318	489
3	0.0233	0.00148	0.0243	18.2	10665	9006	970
4	0.0029	0.00152	0.00392	40.8	22995	19543	2053

(b)The local gate error rate is 10^{-4} .

#purification	X error rate	Z error rate	Merged error rate	Phys. Bell Pair Ineff.	KQ	#single qubit gate	#two qubit gate
0	0.113	0.0976	0.153	1.0	1296	998	149
1	0.0946	0.0153	0.102	2.5	2131	1711	223
2	0.018	0.0102	0.0265	6.2	4147	3434	402
3	0.018	0.00046	0.0184	12.9	7865	6608	734
4	0.000798	0.000433	0.00118	26.8	15626	13236	1426

(c)The local gate error rate is 10^{-5} .

#purification	X error rate	Z error rate	Merged error rate	Phys. Bell Pair Ineff.	KQ	#single qubit gate	#two qubit gate
0	0.109	0.0928	0.151	1.0	1296	998	149
1	0.093	0.0145	0.1	2.5	2120	1702	222
2	0.0179	0.01	0.0263	6.0	4059	3358	395
3	0.0176	0.00034	0.0179	12.4	7636	6413	714
4	0.000589	0.000325	0.000907	25.8	15047	12741	1376